

DCPT/15/86
 FR-PHENO-2015-007
 IPPP/15/43
 LTP 1050
 MPP-2015-154
 19th October 2015

Exclusive J/ψ and Υ photoproduction and the low x gluon

S.P. Jones^{a,b}, A.D. Martin^c, M.G. Ryskin^{c,d} and T. Teubner^e

^a Albert-Ludwigs-Universität Freiburg, Physikalisches Institut, 79104 Freiburg, Germany

^b Max-Planck-Institute for Physics, Föhringer Ring 6, 80805 München, Germany

^c Institute for Particle Physics Phenomenology, University of Durham, Durham DH1 3LE, U.K.

^d Petersburg Nuclear Physics Institute, Gatchina, NRC Kurchatov Institute, St. Petersburg, 188300, Russia

^e Department of Mathematical Sciences, University of Liverpool, Liverpool L69 3BX, U.K.

Abstract

We study exclusive vector meson photoproduction, $\gamma p \rightarrow V + p$ with $V = J/\psi$ or Υ , at NLO in collinear factorisation, in order to examine what may be learnt about the gluon distribution at very low x . We examine the factorisation scale dependence of the predictions. We argue that, using knowledge of the NLO corrections, terms enhanced by a large $\ln(1/\xi)$ can be reabsorbed in the LO part by a choice of the factorisation scale. (In these exclusive processes ξ takes the role of Bjorken- x .) Then, the scale dependence coming from the remaining NLO contributions has no $\ln(1/\xi)$ enhancements. As a result, we find that predictions for the amplitude of Υ production are stable to within about $\pm 15\%$. This will allow data for the exclusive process $pp \rightarrow p\Upsilon p$ at the LHC, particularly from LHCb, to be included in global parton analyses to constrain the gluon PDF down to $x \sim 10^{-5}$. Moreover, the study of exclusive J/ψ photoproduction indicates that the gluon density found in the recent global PDF analyses is too small at low x and low scales.

1 Introduction

The present global PDF analyses (e.g. NNPDF3.0 [1], MMHT2014 [2], CT14 [3]) find that there is a large uncertainty in the low x behaviour of the gluon distribution. There is a lack of very low x data, particularly at low scales. Moreover, the gluon is determined at low x mainly by the DGLAP evolution of deep inelastic scattering, that is, not from a direct measurement¹, but rather from the derivative $dF_2/d\ln Q^2$. As a result, at low scales, the uncertainty on the gluon PDF is large for $x \lesssim 10^{-3}$. On the other hand, the HERA data on diffractive vector meson photoproduction [4, 5, 6, 7, 8, 9, 10, 11, 12, 13, 14, 15], $\gamma p \rightarrow V + p$ and the LHC data on the exclusive processes $pp \rightarrow p V p$ [16, 17, 18] where $V = J/\psi$ or Υ , and $p\text{Pb} \rightarrow p V \text{Pb}$ [19], sample directly the gluon distribution down to $x \sim 10^{-5}$. For a review of exclusive vector-meson production at the LHC see, for example, Ref. [20].

However, J/ψ and Υ data are not used in the global PDF analyses. One reason is that the corresponding cross sections are described by non-diagonal (skewed) analogues of the PDFs, namely generalised parton distributions (GPDs), due to the different masses of the incoming photon and the outgoing V meson [21]. The GPDs can be related to the PDFs via the Shuvaev transform in the low ξ region [22].² In this work, following [23], we make the physically motivated assumption that the input distribution has no singularities in the right-half Mellin- N plane which implies that this relation holds at NLO to accuracy $\mathcal{O}(\xi)$. Another reason is the dependence of the theoretical predictions on the choice of the factorisation scale, μ_F . This problem has two independent parts. One part has a technical nature and the other is more physical. Let us discuss them in turn. First, the ‘technical’ problem, which is related to the convergence of the perturbative expansion at low ξ and low scales. A good illustration is that the NLO amplitude for the exclusive high-energy $\gamma p \rightarrow J/\psi + p$ process [24] was shown to yield a cross section which varies by up to an order of magnitude for a reasonable variation of μ_F . This problem was emphasised recently by Wagner et al. [25]. The strong scale dependence arises because in the DGLAP evolution of low ξ GPDs the probability of emitting a new gluon is strongly enhanced by the large value of $\ln(1/\xi)$. Indeed, the mean number of gluons in the interval $\Delta \ln \mu_F$ is [26]

$$\langle n \rangle \simeq \frac{\alpha_s N_C}{\pi} \ln(1/\xi) \Delta \ln \mu_F^2, \quad (1)$$

leading to a value of $\langle n \rangle$ up to about 8, for the case $\ln(1/\xi) \sim 8$ with the usual μ_F scale variation interval from $\mu_F/2$ to $2\mu_F$. In contrast, the NLO coefficient function allows for the emission of only *one* gluon. Therefore we cannot expect compensation between the contributions coming from the GPD and the coefficient function as we vary the scale μ_F . (At large ξ the compensation is much

¹In principle, measurements of F_L would provide a direct determination, but the data are poor and do not reach low x . Moreover, the convergence of the perturbative series for F_L is relatively poor.

²For GPDs, ξ plays the role of the PDF variable x and is given by $\xi = (p^+ - p'^+)/ (p^+ + p'^+)$, where p^+ and p'^+ are the light-cone plus-momenta of the in- and outgoing protons.

more complete and provides reasonable stability of the predictions to variations of the scale μ_F .) In Section 2, we use the NLO contribution to fix a choice of the factorisation scale for the LO part of the amplitude, which allows the $\ln(1/\xi)$ corrections to be resummed.

The second or ‘physical’ reason why there is a strong scale dependence of J/ψ and Υ photoproduction is due to ‘defects’ in the presently available PDF sets which are obtained in the DGLAP global analyses of deep inelastic and related hard scattering data. That is, our studies indicate that there is a strong scale dependence in vector-meson photoproduction caused by the unexpectedly small LO contribution in comparison with the NLO correction. This occurs due to the very low input gluon density in the low x domain obtained in the recent global PDF analyses. We conclude that at the input scale, the low x gluon density is underestimated in comparison with that for quarks. The crucial observation is that the number of input gluons (which is parametrised *freely* in the global analyses) is found to be much less than the number of such gluons emitted by quarks — or, to be more precise, gluons associated with the quark (each quark carries a gluon field created by its colour charge). With the present global partons the NLO sea quark contribution to V meson photoproduction grows with decreasing x faster than the input gluons. As a result, at sufficiently high energy, the quark component of the NLO correction to V photoproduction approximately cancels the main LO contribution which is due only to the gluon density. Therefore a small variation of the scale in the NLO component leads to a strong variation of the predicted cross section.

Recently the LHCb Collaboration have presented data for open charm and beauty production in the forward direction [27, 28]. These data sample approximately the same kinematic domain as exclusive vector meson production; actually the x values are slightly larger, and the scale for beauty production is also larger. It was shown in [29, 30] that the data can be reproduced by NLO QCD using the present global PDFs. Note, however, that again there is a large sensitivity to the choice of factorization scale. Indeed, to reproduce the data one needs to take a scale approximately a factor of two larger than the natural choice $\mu_F = \sqrt{Q^2 + m_Q^2}$. Since the optimal or appropriate scale for open heavy-quark production is not known at present, these data do not yet reliably determine the low x gluon at low scales. In the present paper we focus on exclusive vector-meson production. Moreover, our goal is not to present a new global PDF analysis or an explicit determination of the low x gluon, but rather to study the possibility to reduce the scale dependence of the prediction, to study the qualitative structure of the NLO amplitude and to give hints of the consequences for the behaviour of the low x gluon at low scales.

In Section 2 we consider the NLO contribution originating from the light quark (singlet) GPD. We show that this part of the NLO amplitude allows us to choose a factorisation scale which sums the $\ln(1/\xi)$ enhanced contributions inside the GPD. The remaining part of the NLO contribution has no large $\ln(1/\xi)$ factors, and, as shown in Section 3.2, the compensation between the scale dependence of the GPDs and of the coefficient functions for Υ production makes the NLO result sufficiently stable for the data to be included in global parton analyses (just as for the predictions of processes at larger x). The study of the J/ψ photoproduction in Section 3.1 suggests that the gluon

density obtained in the existing PDF analyses is too small at low x and low scale. In Section 4 we present our conclusions.

2 NLO corrections and the choice of μ_F

Our aim in this section is to show how knowledge of the NLO contribution for $\gamma p \rightarrow V + p$ allows us to sum the $\ln(1/\xi)$ enhanced contributions by a particular choice of μ_F in the LO part of the amplitude (and correspondingly in the NLO coefficient function), which, in turn, reduces the factorisation scale dependence of the predicted cross section. We outline the procedure in Section 2.2, but first we comment on the NLO formalism.

2.1 NLO formalism for $\gamma p \rightarrow V + p$

The NLO formalism for $\gamma p \rightarrow V p$ has been presented in [24]. However, before we can apply it to describe the high energy V photoproduction data, we must note one important correction.

The LO partonic amplitude, $\mathcal{A}_g^{(0)}(x/\xi)$, for the subprocess $\gamma + (gg) \rightarrow V$, can be calculated by considering the fusion of a photon with a pair of on-shell gluons with zero transverse momentum and physical, transverse, polarisations. If we use dimensional regularisation with $D = 4 + 2\epsilon$ (as in [24]) to regularize the ultraviolet (UV) and infrared (IR) divergences, then the result is given, before dividing by the number of physical transverse polarisations of the incoming gluon, by

$$\mathcal{A}_g^{(0)}(x/\xi) = \alpha_s 2(1 + \epsilon). \quad (2)$$

In D dimensions, there are $D - 2 = 2 + 2\epsilon$ possible transverse directions. Since the entire calculation must be performed in D dimensions, to properly average over the polarisation of the incoming gluon, we must divide (2) by this factor, and not simply by 2. Therefore for the LO partonic amplitude we obtain, contrary to [24] (prior to the first erratum),

$$\mathcal{A}_g^{(0)}(x/\xi) = \alpha_s. \quad (3)$$

The difference of a factor of $(1 + \epsilon)$ does not alter the finite LO result (as ϵ is taken to zero) but does lead to a different NLO result due to the differing counter-terms. Indeed, the extra factor $(1 + \epsilon)$ presented in [24] generates extra terms $\sim \epsilon/\epsilon$ in the counter-terms, Δ , giving them a form

$$\Delta = \dots \left(\frac{1}{\hat{\epsilon}} + 1 + \ln \left(\frac{\mu_F^2}{\mu^2} \right) \right),$$

where $1/\hat{\epsilon} = 1/\epsilon + \gamma_E - \ln(4\pi)$ and γ_E is the Euler-Mascheroni constant. However, with the LO partonic amplitude (3) we instead obtain counter-terms containing

$$\Delta = \dots \left(\frac{1}{\hat{\epsilon}} + \ln \left(\frac{\mu_F^2}{\mu^2} \right) \right).$$

It is precisely this alteration to the counter-terms which leads us to a different NLO finite result.³ This result agrees with that of [24] with both errata.

The details of our recalculation of the NLO result will be published separately [33]. Here we simply state the final result for the high-energy limit of the NLO part of the amplitude. In the high-energy approximation, $W^2 \gg M_V^2$ (where W is the c.m. energy of the incoming γp system and M_V the mass of the vector meson), the imaginary part of the amplitude dominates and the leading contribution to the NLO correction comes from the region $\xi \ll |x| \ll 1$. The matrix element is given by

$$A^{(1)}(\xi, \mu_F) \approx -i\pi C_g^{(0)} \left[\frac{\alpha_s(\mu_R) N_c}{\pi} \ln \left(\frac{m^2}{\mu_F^2} \right) \int_{\xi}^1 \frac{dx}{x} F_g(x, \xi, \mu_F) + \frac{\alpha_s(\mu_R) C_F}{\pi} \ln \left(\frac{m^2}{\mu_F^2} \right) \int_{\xi}^1 dx (F_S(x, \xi, \mu_F) - F_S(-x, \xi, \mu_F)) \right]. \quad (4)$$

Here m is the mass of the c (for J/ψ) or b (for Υ) quark and

$$F_g(x, \xi, \mu) = \sqrt{1 - \xi^2} H_g(x, \xi, \mu), \quad (5)$$

$$F_S(x, \xi, \mu) = \sqrt{1 - \xi^2} H_S(x, \xi, \mu), \quad (6)$$

(for this unpolarised, forward process) with H_g, H_S the gluon and quark singlet GPDs, respectively. The GPDs can be calculated from the diagonal PDFs, $q(x, \mu), \bar{q}(x, \mu)$ and $g(x, \mu)$, via the Shuvaev transforms:

$$H_S(x, \xi, \mu) = \sum_{q=u,d,s} H_q(x, \xi, \mu) - H_q(-x, \xi, \mu), \quad (7)$$

$$H_q(x, \xi, \mu) = \begin{cases} \int_{-1}^1 dx' \left[\frac{2}{\pi} \operatorname{Im} \int_0^1 \frac{ds}{y(s) \sqrt{1 - y(s)x'}} \right] \frac{d}{dx'} \left(\frac{q(x', \mu)}{|x'|} \right), & x \geq 0 \\ \int_{-1}^1 dx' \left[\frac{2}{\pi} \operatorname{Im} \int_0^1 \frac{ds}{y(s) \sqrt{1 - y(s)x'}} \right] \frac{d}{dx'} \left(\frac{\bar{q}(x', \mu)}{|x'|} \right), & x < 0 \end{cases} \quad (8)$$

$$H_g(x, \xi, \mu) = \int_{-1}^1 dx' \left[\frac{2}{\pi} \operatorname{Im} \int_0^1 \frac{ds(x + \xi(1 - 2s))}{y(s) \sqrt{1 - y(s)x'}} \right] \frac{d}{dx'} \left(\frac{g(x', \mu)}{|x'|} \right), \quad (9)$$

where

$$y(s) = \frac{4s(1 - s)}{x + \xi(1 - 2s)}, \quad (10)$$

³This correction was also mentioned in [31, 25] and discussed in more detail in [32].

with an accuracy $\mathcal{O}(\xi)$, see Ref. [23]. Expressions (8) and (9) were used not only for the asymptotic NLO amplitude, (4), but also for the full expression for the complete NLO amplitude used in the numerics presented below. The LO coefficient function,

$$C_g^{(0)} = \alpha_s(\mu_R) \frac{4\pi\sqrt{4\pi\alpha}e_q(e_V^*e_\gamma)}{N_c\xi} \left(\frac{\langle O_1 \rangle_V}{m^3} \right)^{1/2}, \quad (11)$$

where e_i are polarisation vectors and $\langle O_1 \rangle_V$ is the NRQCD (non-relativistic QCD) matrix element of the $c\bar{c} \rightarrow J/\psi$ (or $b\bar{b} \rightarrow \Upsilon$) transition. In order to have a small relativistic correction to $\langle O_1 \rangle_V$, we have to calculate the Feynman diagrams assuming that the charm/bottom-quark line has mass $m = M_V/2$ where $V = J/\psi, \Upsilon$ [34].

One can see directly from the high energy, leading $\ln(1/\xi)$, limit, given in (4), that for the choice $\mu_F = m$ the asymptotic limit of the quark NLO contribution vanishes. It is this observation that will allow us (in Section 2.3) to claim that a suitable value for the factorisation scale in leading logarithm terms is $\mu_F = m$.

Before we show how the NLO contribution allows us to fix the scale μ_F in the LO term, it is informative to first recall its structure and introduce the notation in terms of the LO prediction.

2.2 General procedure

We start with the LO contribution to $\gamma p \rightarrow V + p$. It is sketched in Fig. 1(a), and the amplitude is given by the convolution

$$A^{(0)}(\xi, \mu_F) = \int_{-1}^1 \frac{dx}{x} C_a^{(0)}(x/\xi) F_a(x, \xi, \mu_F) \equiv C_a^{(0)} \otimes F_a(\mu_F), \quad (12)$$

where the sum over $a = q, g$ is understood and $C_q^{(0)} = 0$ for this process. The coefficient function $C_g^{(0)}$ is calculated using the non-relativistic vector meson wave function. In general, the relativistic corrections are not small for the J/ψ case. These corrections should be considered together with the three parton ($c\bar{c}+g$) component of the wave function; that is, accounting for the rôle of gluons which provide the interaction between charm quarks. For this process, it was shown by Hoodbhoy [34] that the consistent treatment of relativistic corrections may, to good accuracy, be effectively accounted for by choosing, in the non-relativistic formula, the charm quark mass $m_c = M_{J/\psi}/2$.⁴ After this, the remaining part of the correction is quite small (a few percent only). So, we may use the non-relativistic J/ψ wave function with $m_c = M_{J/\psi}/2$, to obtain a result with good accuracy.

⁴Strictly speaking, Hoodbhoy considered the electroproduction limit $Q^2 \gg M_{J/\psi}^2$. This limit simplifies the calculation, but inspection of the proof indicates that the statement about a small relativistic correction should be reliable below this limit as well.

We return to discuss $V = J/\psi$ or Υ . At LO the coefficient function $C_g^{(0)}$ does not depend on μ_F , whereas the low x gluon distribution F_g depends strongly on the scale. In other words, based on (12), the exclusive V data measure $g(x, \mu_F)$, but we do not know the value of the scale at which it has been determined. How does this scale freedom arise? To obtain the LO result the coefficient function – the upper box in Fig. 1(a) – is calculated with on-mass-shell gluons with transverse momenta $l_t = 0$. In this collinear approach the factorisation scale μ_F acts effectively as the ultraviolet (UV) cutoff of the logarithmic integral $\int dl_t^2/l_t^2 \propto \ln \mu_F^2$ over the gluon transverse momentum in the gluon loop of Fig. 1(a). Formally, in the LO collinear factorisation approach the value of μ_F is not known. In principle, the full result does not depend on μ_F since the higher-order, NLO, NNLO, ..., corrections compensate the effect of variations of μ_F . However, in reality the perturbative series is truncated and the compensation may not be sufficient to provide the scale stability of the theoretical prediction.

On the other hand, we can go beyond the collinear logarithmic approximation by computing the l_t integral accounting for the l_t dependence⁵ of the hard $\gamma + gg \rightarrow V$ matrix element, \mathcal{M} , shown in the upper box of Fig. 1(a). In comparison with the coefficient function (calculated with $l_t = 0$) now the l_t and l^2 dependence of \mathcal{M} is included explicitly, and provides the UV convergence of the integral over l_t . Formally, in collinear factorisation the difference between the pure logarithmic ($\ln \mu_F^2$) evaluation and the precise calculation of the gluon l_t integral is treated as part of the NLO correction. This part of the NLO correction is of kinematic origin and is usually quite large. Fortunately, it can be moved into the LO component of the amplitude, noticeably reducing the remaining NLO correction.

Instead of performing an independent calculation which accounts for the l_t dependence, we can remain within the collinear approach and determine the value of the l_t integral given that the NLO coefficient function $C_q^{(1)}$ of Fig. 1(b) is known. Indeed, Fig. 1(b) is the only diagram for the quark NLO coefficient function. In this approach the incoming quarks are assumed to be on-mass-shell and with zero transverse momenta but the loop integral over l , which contains the l_t dependence, is calculated exactly. Since this is the same integral as that which occurs in Fig. 1(a) we can use the result for $C_q^{(1)}$ to obtain a precise value, J , of the corresponding integral in the LO amplitude of Fig. 1(a). After this we choose a scale $\mu_F = \mu_0$ which mimics the precise l_t integration. That is, with a scale choice satisfying $\ln \mu_0^2 = J$ we have moved a large contribution from NLO to LO, and can continue to work in the conventional collinear approach, but now with a smaller NLO correction.

⁵A precise integration over l_t was, in particular, implemented in [35].

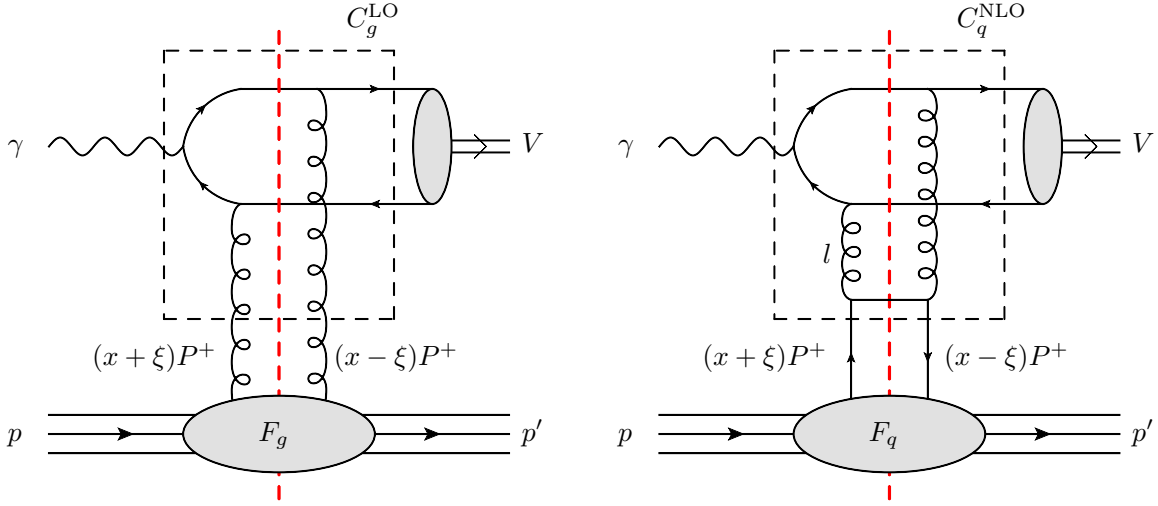


Figure 1: (a) The LO contribution to $\gamma p \rightarrow V + p$, showing the convolution (12). (b) The NLO quark contribution. For these graphs all permutations of the parton lines and coupling of the gluon lines to the heavy-quark pair are to be understood. Here $P \equiv (p + p')/2$ and l is the loop momentum.

2.3 Transfer of part of the NLO to the LO contribution

Since the above observation is crucial, let us demonstrate the procedure in more detail. At NLO level the LO+NLO amplitude at some factorisation scale μ_f may be expressed in the form⁶

$$A^{(0)}(\mu_f) + A^{(1)}(\mu_f) = C^{(0)} \otimes F(\mu_f) + \alpha_s C^{(1)}(\mu_f) \otimes F(\mu_f), \quad (13)$$

where the F s are the GPDs and where the coefficient function $C^{(0)}$ does not depend on the factorisation scale. Note that we are free to evaluate the LO contribution at a different scale μ_F , since the resulting effect can be *compensated* by changes in the NLO coefficient function, which then also becomes dependent on μ_F . Then eq. (13) becomes

$$A^{(0)}(\mu_f) + A^{(1)}(\mu_f) = C^{(0)} \otimes F(\mu_F) + \alpha_s C_{\text{rem}}^{(1)}(\mu_F) \otimes F(\mu_f). \quad (14)$$

Note that although the first and second terms on the right hand side depend on μ_F , their sum does not (to $\mathcal{O}(\alpha_s^2)$) and is equal to the full LO+NLO amplitude calculated at the factorisation scale μ_f .

In (13) the NLO coefficient function $C^{(1)}$ is calculated from Feynman diagrams which are independent of the factorisation scale. How does the μ_F dependence of $C_{\text{rem}}^{(1)}$ in (14) actually arise? It occurs because we must subtract from $C^{(1)}$ the α_s term which was already included in the LO contribution.⁷ Since the LO contribution was calculated up to some scale μ_F the value of $C^{(1)}$ after

⁶For ease of understanding we omit the parton labels $a = g, q$ on the quantities in (13) and the following equations. The matrix form of the equations is implied.

⁷Simultaneously this subtraction also provides the infrared convergence of $C^{(1)}$.

the subtraction depends on the value μ_F chosen for the LO component. The change of scale of the LO contribution from μ_f to μ_F also means we have had to change the factorisation scale which enters the coefficient function $C^{(1)}$ from μ_f to μ_F . The effect of this scale change is driven by the LO DGLAP evolution, which is given by

$$A^{(0)}(\mu_F) = \left(C^{(0)} + \frac{\alpha_s}{2\pi} \ln \left(\frac{\mu_F^2}{\mu_f^2} \right) C^{(0)} \otimes V \right) \otimes F(\mu_f), \quad (15)$$

where V denotes the skewed splitting functions. That is, by choosing to evaluate $A^{(0)}$ at scale μ_F we have moved the part of the NLO (i.e. α_s) corrections given by the last term of (15) from the NLO to the LO part of the amplitude. In this way $C^{(1)}$ becomes the remaining μ_F -dependent coefficient function $C_{\text{rem}}^{(1)}(\mu_F)$ of (14). In spite of the unusual form of (14), with two different scales μ_f and μ_F , it is an exact equality at NLO and could, in principle, be generalised to higher orders.⁸

2.4 Large $\ln(1/\xi)$ terms resummed in the LO contribution

The idea is to use the above procedure to reduce the scale dependence of the exclusive V photoproduction amplitude. Unfortunately the value of μ_F is just one number, while $C^{(1)}(x/\xi)$ is a function of the ratio x/ξ . So we have no chance to nullify $C^{(1)}$ completely. Nevertheless we can nullify the most important NLO correction which is enhanced by the large value of $\ln(1/\xi)$. This contribution is generated by the integral $\int(dx/x)$ in the $C_{\text{rem}}^{(1)}(x/\xi, \mu_F)F(x, \xi, \mu_f)$ convolution of eq. (14) over the kinematic region of $1 \gg x \gg \xi$. That is, we choose a scale $\mu_F = \mu_0$ which nullifies $C^{(1)}(x/\xi)$ in the limit of $x \gg \xi$. It can be seen from (4) that the scale $\mu_F = \mu_0 = m$ ensures that the $\ln(1/\xi)$ -enhanced NLO corrections completely vanish for both the quark and the gluon components.

From the NLO viewpoint the particular choice of $\mu_F = m$ in the LO part is irrelevant. The corresponding order α_s effect is exactly compensated by the remaining $C_{\text{rem}}^{(1)}$ term. However, the variation of μ_F in the LO part affects not only the $\mathcal{O}(\alpha_s)$ terms but the higher-order α_s contributions as well. Therefore, in this way, we resum the important large $\ln(1/\xi)$ -enhanced part of the higher-order α_s corrections inside the parton distribution convoluted with the LO coefficient function and improve the convergence of the perturbative series.⁹

Actually our approach is rather close in spirit to the k_t -factorisation method. Indeed, there, the value of the factorisation scale is driven by the structure of the $k_t = l_t$ (or the virtuality, Q^2) integral

⁸For example, if the NNLO contribution were known, then we will have three scales: μ_f , $\mu_F \equiv \mu^{\text{LO}}$, and μ^{NLO} , where the NNLO correction to (14) takes the form $\alpha_s^2 C_{\text{rem}}^{(2)}(\mu^{\text{LO}}, \mu^{\text{NLO}}) \otimes F(\mu_f)$. The scale μ^{NLO} is fixed to nullify this term in the limit $x \gg \xi$, and hence further reduce the sensitivity to variations of the scale μ_f .

⁹In particular, the most important factorisation scale dependence, enhanced by large $\ln(1/\xi)$, is caused by the double log terms, $[\alpha_s \ln(\mu_F) \ln(1/x)]^n$, generated in the axial gauge by ladder-type diagrams. For GPDs this ladder contribution was studied in [36], where it was shown, in the large $\ln(1/x)$ limit, that the skewed splitting functions

in the diagrams of Fig. 1.¹⁰ In the k_t -factorisation approach this k_t integral is written explicitly, while the parton distribution *unintegrated* over k_t is generated by the last step of the DGLAP evolution, similar to the prescription proposed in Refs. [37, 38]. Now, using the known NLO result, we account for the *exact* k_t integration in the last cell adjacent to the LO hard matrix element. This hard matrix element \mathcal{M} , shown in the upper box of Fig. 1(a), provides the convergence of the integral at large k_t . In this way it puts an effective upper limit of the k_t integral, which plays the role of an appropriate factorisation scale.

The details of the prescription, for the case of the high-energy Drell-Yan process, were discussed in [39]. Indeed, Drell-Yan production of low-mass lepton pairs at high rapidity is another process for which the NLO prediction depends sensitively on the choice of the factorisation scale, unless the $\ln(1/x)$ enhancements are first resummed in the incoming parton distributions. It was found in Ref. [39] that, after the scale $\mu_F = \mu_0$ is fixed for the LO contribution, the variation of the scale in the remaining NLO part does not noticeably change the predicted Drell-Yan cross section. In [39] it was shown how to calculate μ_0 for the Drell-Yan process and, moreover, that the NLO prediction with $\mu_F = \mu_0$ is very close to the NNLO result.

Returning to the earlier discussion in this subsection, it is clear from (4) and (14) that the scale choice $\mu_F = m = M_V/2$ provides the appropriate resummation of the $\ln(1/\xi)$ enhanced terms, and, as a consequence, suppresses the remaining high-energy NLO corrections. In other words, the GPDs with $\mu_F = m$ (chosen in the LO part) include all the $\ln(1/\xi)$ enhanced contributions, while the remaining NLO corrections arise only from hard matrix elements corresponding to intermediate states of relatively small mass of about M_V .

We can also explain this pictorially. As noted above, the μ_F dependence of the NLO correction is caused by the subtraction of the contribution generated by the evolution equation. In particular, the correction which (i) depends on μ_F and (ii) is enhanced by $\ln(1/\xi)$, is generated by the ladder-type diagrams¹¹ shown in Fig. 2. The choice of the factorisation scale μ_{F_i} determines which part of the diagram is attributed to the evolution of the PDF and which to the hard matrix element. By choosing the value of $\mu_F = \mu_0 = M_V/2$ we include all the ladder cells in the LO part, so that

are proportional to $1/x$. So these double log terms come from DGLAP integrals of the form

$$\left(\int^{\mu_F^2} \frac{dk_n^2}{k_n^2} \int^{k_n^2} \frac{dk_{n-1}^2}{k_{n-1}^2} \cdots \int^{k_2^2} \frac{dk_1^2}{k_1^2} \right) \left(\int_x^1 \frac{dx_n}{x_n} \int_{x_n}^1 \frac{dx_{n-1}}{x_{n-1}} \cdots \int_{x_2}^1 \frac{dx_1}{x_1} \right) \sim [\alpha_s \ln(\mu_F) \ln(1/x)]^n / (n!)^2$$

where we have strong $k^2 \equiv k_t^2$ and x ordering. Thanks to the strong k_t and x ordering in these double log LO integrals, the correct upper limit, μ_F , in the first integral automatically provides the exact resummation of all the terms in the double log series.

¹⁰We stress again that, in the high energy ($x \gg \xi$) contribution, the form of the integral over the gluon loop momentum l_t is exactly the same in both the quark (Fig. 1(b)) and gluon (Fig. 1(b) but with the quark lines replaced by gluons) NLO contributions. Therefore the scale $\mu_F = \mu_0$ simultaneously nullifies the high energy quark and gluon contributions. Note that this is only true after the corrections discussed in Section 2.1 are included.

¹¹Ladder diagrams occur in the axial gauge which is conventionally used to calculate the GPDs.

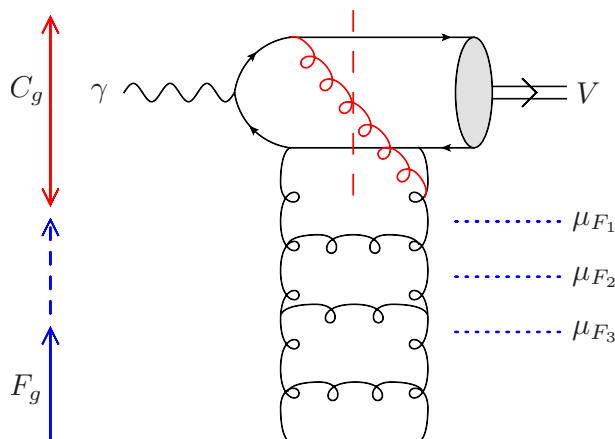


Figure 2: A Feynman diagram which illustrates different possibilities for the division of cells between the parton evolution and the hard matrix element, dependent on the choice of the factorisation scale, μ_{F_i} .

the remaining NLO matrix element will not receive any contribution from ladder-type diagrams (at small ξ). Note that the ladder diagrams would contribute to the NLO matrix element (from μ_F to μ_0) if we were to choose a scale $\mu_F < \mu_0$. For the choice $\mu_F > \mu_0$ the NLO matrix element would contain the ladder diagrams with the negative sign in order to compensate the extra contributions (from μ_0 to μ_F) included in the LO part.

Since we consider an exclusive process, the mass of the final state is fixed, but the intermediate states, corresponding to the discontinuity which gives the imaginary part of the amplitude (depicted using a dotted line in Fig. 2), depend on the choice of scale. For larger values of μ_F the mass of the allowed intermediate states in the matrix element becomes smaller. Of course, it is impossible to absorb inside the evolution all intermediate states other than the heavy quark pair $Q\bar{Q}$ state which produces the V ; for example we cannot absorb the effects of the uppermost gluon in Fig. 2 emitted by the upper heavy quark. Nevertheless, when we choose the appropriate scale $\mu_F = M_V/2$, the mass of the remaining intermediate states becomes of the order of M_V . This choice will move $\ln(1/\xi)$ contributions from the matrix element into the GPD. It will therefore provide a much more stable final result, since the remaining NLO contributions then cannot be enhanced by the large values of $\ln(1/\xi)$.

It should be emphasised that the asymptotics of the NLO amplitude is used only to determine the effective scale μ_F . In all our further numerics we use the full expression for the complete NLO amplitude as given in [24, 32, 33].

3 Can exclusive vector meson production data be included in a global PDF fit?

In this section we present our results for the exclusive $\gamma p \rightarrow J/\psi + p$ and $\gamma p \rightarrow \Upsilon + p$ processes as functions of the factorisation scale μ_f , and the renormalisation scale μ_R . The cross section relies sensitively on the gluon PDF at small x , in a kinematic regime where it is very poorly known, as well as depending of the choice of scales. For these quasi-elastic processes we present just the dominant imaginary part of the amplitude. The real part of the coefficient functions has been calculated exactly, both via a dispersion relation [24] and by directly computing the real part of the loop integrals [32, 33], it is non-zero in the time-like region $|x| < \xi$. Therefore, to compute the real part of the amplitude directly, we need also the GPDs in this region. Unfortunately, the Shuvaev transform is not valid in the time-like region [23]. Nevertheless, the real part of the amplitude can be included via dispersive methods on the level of the amplitude. However, giving a prediction of the full cross section is not our objective here. Rather our aim is to study the stability of the perturbative predictions and to investigate whether or not we can determine optimum scales so that experimental data for these processes, and the related $pp \rightarrow pVp$ processes, can be included in global PDF (collinear) analyses to constrain the gluon PDF at low x , in a domain for which, at present, there are no data. For this goal it is sufficient to work with the more simple imaginary part of the amplitude.

We recall the main result of Section 2. We start from the key equation, (14), that is

$$A^{(0)}(\mu_f) + A^{(1)}(\mu_f) = C^{(0)} \otimes F(\mu_F) + \alpha_s C_{\text{rem}}^{(1)}(\mu_F) \otimes F(\mu_f). \quad (16)$$

To obtain this result we had introduced by hand a new scale μ_F in the LO term and showed that the choice $\mu_F = m = M_V/2$ allowed us to resum and transfer all the enhanced large $\ln(1/\xi)$ terms from the NLO contribution to the LO term, leaving a much smaller remaining NLO contribution $\alpha_s C_{\text{rem}}^{(1)}(\mu_F) \otimes F(\mu_f)$. There is still a μ_f scale dependence, but now this should be much weaker.

3.1 The process $\gamma p \rightarrow J/\psi + p$

To obtain predictions for exclusive J/ψ photoproduction we are working at scales close to the input GPDs used in the calculation. The results for the scale variation of the imaginary part of the amplitude are shown in the two plots of Fig. 3. In each plot we show separately the LO and NLO contributions to the amplitude.¹² The left plot shows how these contributions change if we vary all the scales $\mu_f = \mu_F = \mu_R \equiv \mu$ simultaneously, taking $\mu^2 = m^2/2, m^2, 2m^2$. In the right plot we

¹²We choose to use CTEQ66 partons [40] since the gluon obtained is positive definite and since they were used in our earlier works on the subject [41, 35]. Moreover, since we are emphasising the general procedure rather than making quantitative predictions, the choice of any particular, reasonable PDF set is not important.

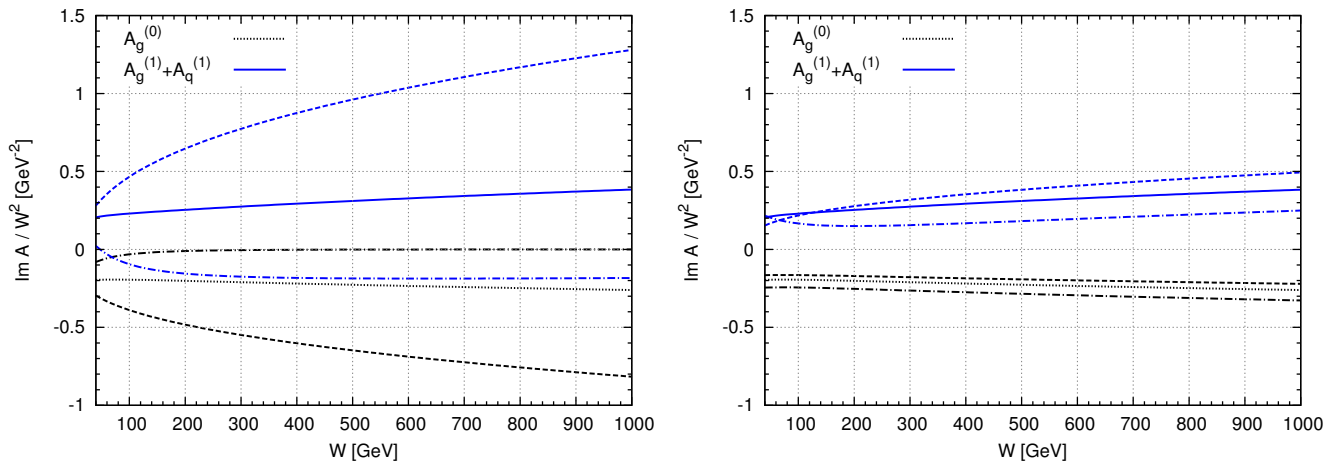


Figure 3: Predictions of $\text{Im}A/W^2$ for $\gamma p \rightarrow J/\psi + p$ as a function of the γp centre-of-mass energy W , produced using CTEQ6.6 partons [40] with scales $\mu \equiv \mu_F = \mu_f = \mu_R$ (left panel) and $\mu \equiv \mu_f = \mu_R$ with $\mu_F^2 = 2.4 \text{ GeV}^2$ (right panel). The bottom (top) set of curves corresponds to the Born (1-loop) contribution with the scale variation $\mu^2 = 1.2, 2.4, 4.8 \text{ GeV}^2$. The dot-dashed, solid and dashed lines correspond to the low, central and high values of the scale μ , respectively. Note that for the left panel, the bands overlap for energies bigger than about 70 GeV.

fix μ_F at the optimum scale $\mu_F = m$ and vary $\mu_f = \mu_R \equiv \mu$. The result is dramatic. The transfer of the $\ln(1/\xi)$ terms from the NLO to the LO contribution has significantly reduced the μ_f scale dependence.

But there is another, more severe problem. The LO contribution is dominated by the NLO contribution of opposite sign. Thus the imaginary part of the quasi-elastic $\gamma p \rightarrow J/\psi + p$ amplitude changes sign when the NLO contribution is added. As it stands, this result is in contradiction with modelling the interaction as an elastic forward scattering where the imaginary part of the amplitude is positive. What is happening? The explanation is interesting. In general, the global DGLAP PDF analyses start from input forms which are completely arbitrary and, moreover, neglecting any constraints, know nothing about the structure of the evolution at low Q^2 . It is then found that the gluon PDF tends to be small, or even negative, in the low Q^2 , low x ($10^{-4} \lesssim x \lesssim 10^{-2}$) domain, see Fig. 4. Clearly due to the lack of data constraints in this domain the gluon is not reliably known.

Let us study the over-simplified case with an input gluon $g(x) = 0$ so that at the input scale we have only quark PDFs. For $\gamma p \rightarrow J/\psi + p$ the quark contribution only appears at NLO. The imaginary part of this NLO contribution is negative with respect to the normal ($g \neq 0$) LO term. Indeed, when calculating the NLO coefficient function we must subtract the contribution which is already generated by LO evolution. However, the subtraction is performed purely formally in order to avoid the infrared divergence and *does not* account for the actual value of the gluon density used

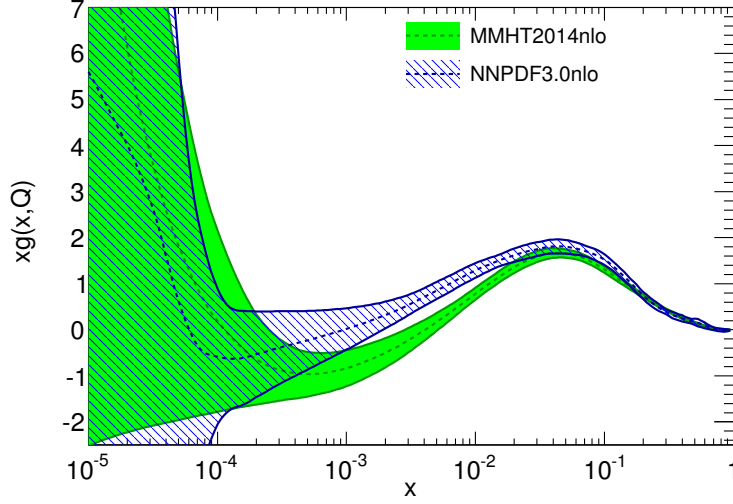


Figure 4: The gluon distribution at $Q^2 = 1.21 \text{ GeV}^2$ as determined by two recent global analyses [1, 2]. Figure produced using [42, 43].

to calculate the LO term. Therefore, at low scales, where the LO term is suppressed by much too small ‘unphysical’ gluon PDFs obtained from the global fits, the NLO term generated by the quark is not just a correction, but is the dominant contribution. As a consequence, the imaginary part of the quasi-elastic amplitude becomes negative (in comparison with the LO contribution) and the observed behaviour reveals a lack of stability of the perturbative series at this order. Of course, at high scales where evolution, and not the input, determine the PDFs, we obtain a sensible NLO prediction.

This simple consideration demonstrates that if $\gamma p \rightarrow J/\psi + p$ and $pp \rightarrow p + J/\psi + p$ data could be included in a global fit, then they would put a strong constraint on the low x input gluon distribution. It is not simply that $g(x)$ must be positive, but that actually the input gluons cannot be smaller than the density of gluons emitted by the quarks before the beginning of the evolution, when the parton virtuality $Q < Q_0$. If J/ψ data would have been included in the collinear global parton analyses, this constraint on the low x input gluon would have been automatically satisfied.

Indeed, it is seen from the second plot of Fig. 3 that after the $\ln(1/\xi)$ enhanced corrections are resummed by fixing $\mu_F = m$, the stability of both the LO and the NLO components of the amplitude under the scale variations are much better. From this viewpoint the J/ψ data may be included in a global PDF analysis. The only problem is that the gluon density obtained in the existing PDF analyses is too small at input scales and low x ($10^{-5} \lesssim x \lesssim 10^{-2}$), so that we get the wrong sign of the imaginary part of the amplitude. This means that if J/ψ data were included in

the global PDF analyses, we must get a larger gluon density at low scales.¹³ Larger gluons in this kinematic domain will increase the LO component of the J/ψ photoproduction amplitude and will provide the correct sign for the whole LO+NLO amplitude.

3.2 The processes $\gamma p \rightarrow \Upsilon + p$ and $pp \rightarrow p\Upsilon p$

The top two plots of Fig. 5 show the results for the scale sensitivity of $\gamma p \rightarrow \Upsilon + p$, analogous to those of Fig. 3 for $\gamma p \rightarrow J/\psi + p$. Again we see that fixing the scale $\mu_F = M_\Upsilon/2$ reduces the μ_f scale uncertainty. The lower two plots show that part of this stability arises because the change caused by variation of μ_R is to some extent compensated by an ‘opposite’ change due to the variation of μ_f . If we were to choose a non-optimal scale, say for example, $\mu_F^2 = 2m^2$, then the scale variation turns out to be about twice as large as for the optimal choice $\mu_F^2 = m^2$. Due to the larger Υ mass we are now working at scales with more perturbative stability. The LO contribution is partly cancelled by the NLO term, but is not dominated by it. If we take the upper right or lower left plot of Fig. 5 then the μ_f scale uncertainty of the amplitude is about $\pm 15\%$ and $\pm 25\%$ respectively. As a result the data for exclusive Υ production can be used in global PDF analyses to probe the gluon distribution down to $x \sim 10^{-5}$, in the case of LHCb kinematics. The calculation of exclusive $pp \rightarrow p\Upsilon p$ is described in [35]. It is based on the sum of the two diagrams shown in Fig. 6. For an Υ produced at large rapidity y , the dominant contribution is from the diagram with the larger γp centre-of-mass energy W_+ , which depends on the gluon density at $x \simeq M_\Upsilon e^{-y}/\sqrt{s}$. The small contribution from the other diagram, with much lower energy W_- , may be estimated from the existing HERA data.

If we use the central values of the presently available PDF sets obtained from global analyses, then we find cross section predictions which are about a factor of four below the HERA exclusive Υ data [6, 14, 15]. This indicates that future PDF global analyses with Υ data included will, just as for J/ψ data, require a larger gluon distribution at low values of x . While the exclusive Υ process samples the PDFs at scales $Q^2 \sim M_\Upsilon^2/4$, the larger gluon required at these Q^2 will affect the gluon densities at all values of Q^2 via the evolution.

3.3 Note on the alternative k_t -factorisation approach

The collinear DGLAP global analyses tend to result in gluon distributions with valence-like x distributions at low scales, see Fig. 4. On the other hand, the approach used in the JMRT paper [35], to study exclusive vector meson production, is free from this problem. There, the ‘NLO’ prediction was not calculated as a correction from NLO Feynman diagrams in collinear factorisation, but

¹³Most probably the pure DGLAP global analyses should take into account absorptive corrections, which are not negligible at low x and low Q^2 . The existing very small gluon densities in this kinematic domain are a way of mimicking these absorptive effects.

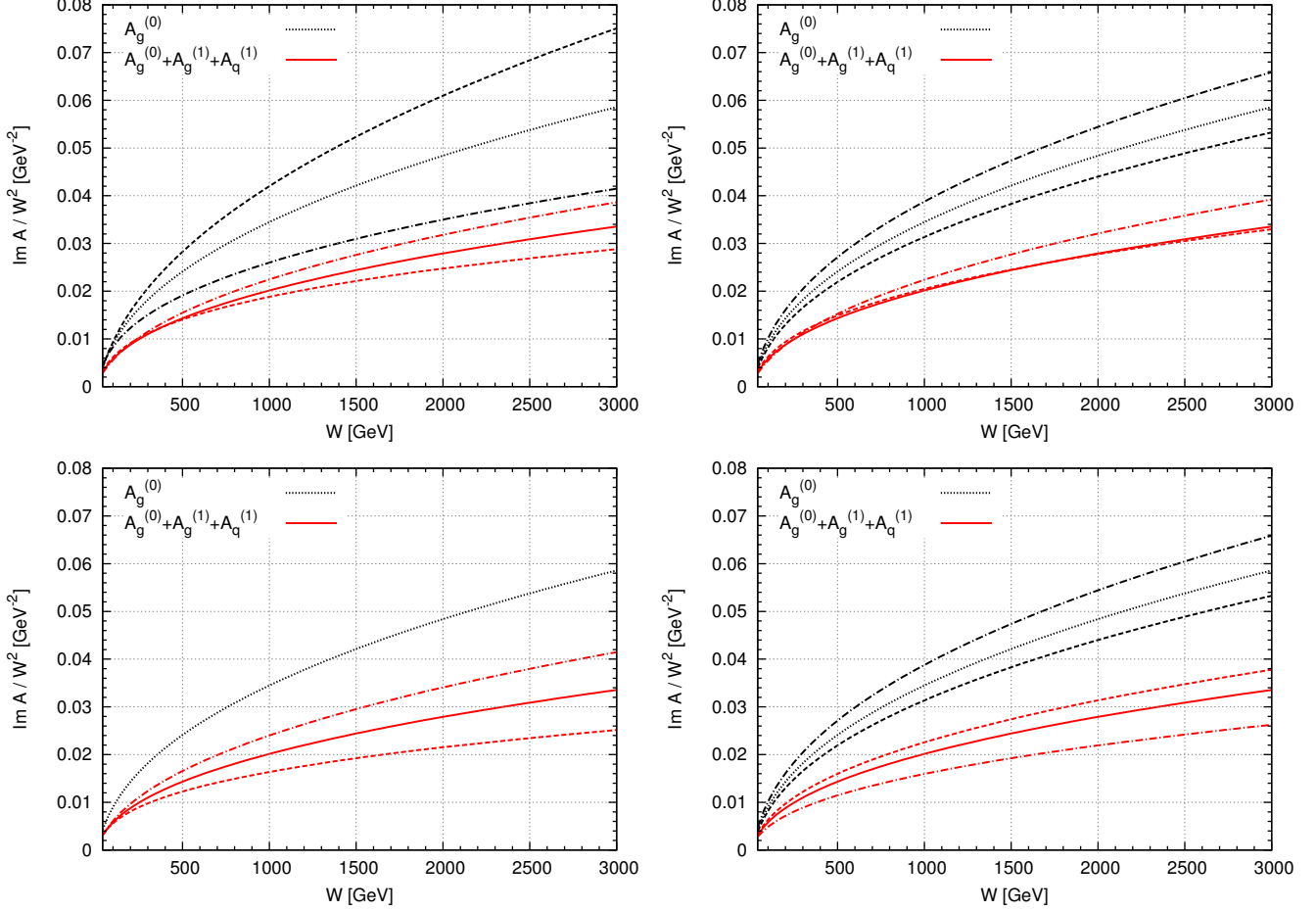


Figure 5: Predictions of $\text{Im}A/W^2$ for $\gamma p \rightarrow \Upsilon + p$ as a function of the γp centre-of-mass energy W , produced using CTEQ6.6 partons [40]. The scales are $\mu \equiv \mu_F = \mu_f = \mu_R$ (top left), $\mu \equiv \mu_f = \mu_R$ with $\mu_F^2 = 22.4 \text{ GeV}^2$ (top right), $\mu \equiv \mu_f$ with $\mu_F^2 = \mu_R^2 = 22.4 \text{ GeV}^2$ (bottom left), $\mu \equiv \mu_R$ with $\mu_f^2 = \mu_F^2 = 22.4 \text{ GeV}^2$ (bottom right). The top (bottom) set of curves corresponds to the LO (LO+NLO) contribution with the scale variation $\mu^2 = 11.9, 22.4, 44.7 \text{ GeV}^2$. The dot-dashed, solid and dashed lines correspond to the low, central and high values of the scale μ , respectively. The large GPD uncertainties are not shown.

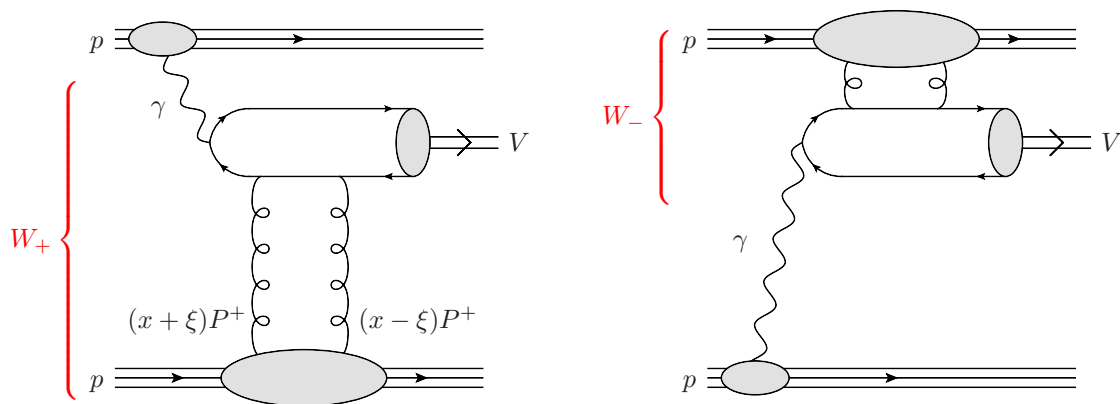


Figure 6: The two diagrams describing exclusive Υ production at the LHC. Diagram (a), the W_+ component, is the dominant contribution for an Υ produced at large rapidity y . Thus data for $pp \rightarrow p\Upsilon p$ allow a probe of very low x values, $x \simeq M_\Upsilon e^{-y}/\sqrt{s}$; recall that in the (dominant) imaginary part of the Born amplitude we have $x = \xi$.

approximated by taking the full integral over the gluon k_t in Fig. 1(a), including an ansatz for the now k_t dependent gluon. The convergence of this explicit k_t integral provides effectively the ‘optimal’ value of the factorisation scale and in this way sums all $\ln(1/\xi)$ enhanced terms, accounting for a large part of the NLO corrections. It does, of course, not include corrections from diagrams which do not have a ladder structure, however, the contribution from the light quarks, Fig. 1(b), is already included in the unintegrated gluon distribution used in JMRT [35]. Clearly, then the quasi-elastic amplitude is positive definite. Let us briefly describe how our ‘NLO’ predictions for $\gamma p \rightarrow \Upsilon + p$ data were made. First the incoming gluon distribution was fitted, within this approach and using an ansatz for the gluon based on the important double-logarithmic dependence on $\ln(1/x)$ and $\ln Q^2$, to reproduce the J/ψ data from HERA and the LHC. Then we proceeded to Υ production using our fitted gluon. We verified that, in the relevant kinematic domain, this gluon reproduces the NLO DGLAP evolution to good accuracy. Therefore it was not surprising that the ‘NLO’ *predictions* for the Υ cross section, as a function of W , agreed well with the LHCb data [18] when they became available.

4 Conclusions

Here we have been concerned about the inclusion of exclusive vector meson production data in global PDF analyses in order to probe the gluon density at small values of x ; that is, in the $x \lesssim 10^{-4}$ domain. Note that in this domain the input gluon PDF is freely parametrized, and is found to have a tendency to be valence-like with large uncertainties. It was hoped that the situation would be

changed as data for exclusive vector meson production, $V = J/\psi$ and Υ , which are very sensitive to the gluon at small x , became available at HERA and the LHC; particularly measurements of the exclusive process $pp \rightarrow pVp$ at the LHC with V detected at large rapidity. Why has this not happened (so far)?

For J/ψ , the main problem is, at first sight, the very poor convergence of the perturbative expansion in the collinear approach. This can be seen, e.g., from Fig. 3, where the NLO contribution is comparable to the LO term and opposite in sign. However, we argued that this large NLO contribution, in comparison with that of the LO, reflects not the poor convergence, but rather that the global PDF analyses find a gluon density which is too small at low x and low scales. For this reason we find a LO contribution to exclusive J/ψ photoproduction amplitude which is too small. We argued that the input gluon in the collinear approach, used in the global PDF analyses, should not be parametrized freely, but should be subject to some constraints. We noted that working in the physical, k_t -factorisation type scheme would avoid these problems.

For exclusive Υ production the situation is much better. We found that the optimum factorisation scale is much higher, the perturbative expansion at NLO in collinear factorisation converges well, and the remaining mild scale dependence of the predictions ($\sim \pm 15\%$ on amplitude level) means that data for $pp \rightarrow p\Upsilon p$ can now be included in the global PDF fits to determine the gluon in the low x regime for the first time.

It is appropriate to list the theoretical uncertainties of the present calculation. Although the leading double log terms have been resummed correctly to all orders, there still exist remaining NNLO and higher contributions, which are unknown at present. When the full NNLO amplitude is known we showed how the scale uncertainty can be further reduced. Next, we consider the accuracy of the expressions which relate GPDs to conventional PDFs, (8) and (9). These relations are based on conformal invariance and the equality of the Gegenbauer moments of GPDs to the Mellin moments of PDFs. Due to the polynomial property [21] the accuracy of this equality of the moments is $\mathcal{O}(\xi^2)$, providing an $\mathcal{O}(\xi)$ accuracy for (8) and (9), see [23]. However, recall that the Shuvaev transform *assumes* the absence of the singularities in the right-half Mellin- N plane for the input distribution. This assumption is physically reasonable since in the Regge approach there are no singularities in the right-half ($j > 1$) plane in the space-like ($|x| > \xi$) domain where we actually work. Nevertheless, whenever possible, this assumption should be checked. One check is that the predictions for the GPD/PDF ratio obtained in this way are in a good agreement (especially for low x gluons, which are the most important for exclusive J/ψ or Υ production) with the NLO results of [44] coming from a fit to deeply virtual Compton scattering (DVCS) HERA data. Finally, the relativistic correction to the vector meson wave function, which is discussed in Section 2.2, is not expected to be significant [34].

We noted that an alternative probe of the low x gluon at low scales has been considered in [29, 30]. There they study the data for charm (and beauty) production obtained in the forward

direction by the LHCb Collaboration [27, 28]. Again it is found that the predictions strongly depend on the choice of factorization scale. Their prediction is lower than the data if the natural scale $\mu_F^2 = m_Q^2 + p_t^2$ is chosen, and it is found that a larger μ_F is needed to reproduce the data using the existing global PDFs. Thus our expectation of a larger gluon at low x is not in contradiction with the LHCb charm (and beauty) forward data.

Acknowledgements

MGR thanks the IPPP at Durham University for hospitality. MGR is supported by the RSCF grant 14-22-00281. SPJ is supported by the Research Executive Agency (REA) of the European Union under the Grant Agreement PITN-GA2012316704 (HiggsTools), and TT is supported by STFC under the consolidated grant ST/L000431/1.

References

- [1] R.D. Ball *et al.* [NNPDF Collaboration], JHEP **1504** (2015) 040.
- [2] L.A. Harland-Lang, A.D. Martin, P. Motylinski and R.S. Thorne, Eur. Phys. J. **C75** (2015) 5, 204.
- [3] S. Dulat, T.J. Hou, J. Gao, M. Guzzi, J. Huston, P. Nadolsky, J. Pumplin and C. Schmidt *et al.*, arXiv:1506.07443 [hep-ph].
- [4] S. Aid *et al.* [H1 Collaboration], Nucl. Phys. **B468** (1996) 3-36.
- [5] S. Aid *et al.* [H1 Collaboration], Nucl. Phys. **B472** (1996) 3-31.
- [6] C. Adloff *et al.* [H1 Collaboration], Phys. Lett. **B483** (2000) 23-35.
- [7] A. Aktas *et al.* [H1 Collaboration], Eur. Phys. J. **C46** (2006) 585-603.
- [8] C. Alexa *et al.* [H1 Collaboration], Eur. Phys. J. **C73** (2013) 2466.
- [9] M. Derrick *et al.* [ZEUS Collaboration], Phys. Lett. **B350** (1995) 120-134.
- [10] J. Breitweg *et al.* [ZEUS Collaboration], Z. Phys. **C75** (1997) 215-228.
- [11] J. Breitweg *et al.* [ZEUS Collaboration], Eur. Phys. J. **C6** (1999) 603-627.
- [12] S. Chekanov *et al.* [ZEUS Collaboration], Eur. Phys. J. **C24** (2002) 345-360.

- [13] S. Chekanov *et al.* [ZEUS Collaboration], Nucl. Phys. **B695** (2004) 3-37.
- [14] J. Breitweg *et al.* [ZEUS Collaboration], Phys. Lett. **B437** (1998) 432-444.
- [15] S. Chekanov *et al.* [ZEUS Collaboration], Phys. Lett. **B680** (2009) 4-12.
- [16] R. Aaij *et al.* [LHCb Collaboration], J. Phys. **G40** (2013) 045001.
- [17] R. Aaij *et al.* [LHCb Collaboration], J. Phys. **G41** (2014) 055002.
- [18] R. Aaij *et al.* [LHCb Collaboration], arXiv:1505.08139 [hep-ex].
- [19] B. Abelev *et al.* [ALICE Collaboration], Phys. Rev. Lett. **133** (2014) 23, 232504.
- [20] A.J. Baltz *et al.*, Phys. Rept. **458** (2008) 1.
- [21] X-D. Ji, J. Phys. **G24** (1998) 1181.
- [22] A.G. Shuvaev, Phys. Rev. **D60** (1999) 116005.
- [23] A.D. Martin, C. Nockles, M.G. Ryskin, A.G. Shuvaev and T. Teubner, Eur. Phys. J. **C63** (2009) 57-67.
- [24] D.Yu. Ivanov, A. Schäfer, L. Szymanowski and G. Krasnikov, Eur. Phys. J. **C34** (2004) 3, 297, *Erratum ibid.* **C75** (2015) 2, 75, *Erratum* arXiv:hep-ph/0401131v3.
- [25] D.Yu. Ivanov, B. Pire, L. Szymanowski and J. Wagner, AIP Conf. Proc. **1654** (2015) 090003.
- [26] Y.L. Dokshitzer, D. Diakonov and S. Troian, Phys. Rept. **58** (1980) 269-395.
- [27] R. Aaij *et al.* [LHCb Collaboration], Nucl. Phys. **B871** (2013) 1.
- [28] R. Aaij *et al.* [LHCb Collaboration], JHEP **1308** (2013) 117.
- [29] O. Zenaiev *et al.*, Eur. Phys. J. **C75** (2015) 396.
- [30] R. Gauld, J. Rojo, L. Rottoli and J. Talbert, arXiv:1506.08025 [hep-ph]
- [31] C. Nockles, *Diffraction Processes and Parton Distribution Functions in the Small x Regime*, PhD thesis, University of Liverpool, August 2009 (unpublished).
- [32] S.P. Jones, *A Study of Exclusive Processes to NLO and Small- x PDFs from LHC Data*, PhD thesis, University of Liverpool, September 2014 (unpublished).
- [33] J. Gracey, S.P. Jones and T. Teubner, in preparation.
- [34] P. Hoodbhoy, Phys. Rev. **D56** (1997) 388.

- [35] S.P. Jones, A.D. Martin, M.G. Ryskin and T. Teubner, JHEP **1311** (2013) 085.
- [36] J. Bartels and M. Loewe, Z. Phys. **C12** (1982) 263.
- [37] M.A. Kimber, A.D. Martin and M.G. Ryskin, Phys. Rev. **D63** (2001) 114027.
- [38] A.D. Martin, M.G. Ryskin and G. Watt, Eur. Phys. J. **C66** (2010) 163.
- [39] E.G. de Oliveira, A.D. Martin and M.G. Ryskin, Eur. Phys. J. **C72** (2012) 2069.
- [40] Q. Cao, J. Huston, H. Lai, P.M. Nadolsky, J. Pumplin, W. Tung, D. Stump and C.-P. Yuan, Phys. Rev. **D78** (2008) 013004.
- [41] A.D. Martin, C. Nockles, M.G. Ryskin and T. Teubner, Phys. Lett. **B662** (2008) 252-258.
- [42] V. Bertone, S. Carrazza and J. Rojo, Comput. Phys. Commun. **185** (2014) 1647-1668, [arXiv:1310.1394 \[hep-ph\]](#).
- [43] S. Carrazza, A. Ferrara, D. Palazzo and J. Rojo, J. Phys. **G42** (2015) 057001, [arXiv:1410.5456 \[hep-ph\]](#).
- [44] K. Kumericki and D. Muller, Nucl. Phys. **B841** (2010) 1.